Proceeding of the 2004 American Control Conference
Boston, Massachusetts June 30 - July 2, 2004

Optimal decoupling for MIMO-controller design with robust performance

D.Vaes, J. Swevers and P. Sas
KULeuven, Department of Mechanical Engineering, Division PMA
Celestijnenlaan 300B, B-3001 Heverlee, Belgium
david.vaes@mech.kuleuven.ac.be

***Abstract*— MIMO-identification and robust MIMO-controller design are cumbersome. As a result, MIMO-systems are often controlled by decentralized control systems, which consist of independent SISO-controllers based on the diagonal elements of the system. The neglected off-diagonal elements limit however the performance. This paper presents a design approach that combines decentralized control design with an input/output decoupling transformation yielding higher closed loop performance. This approach consists of a procedure to find the transformations of the inputs and the outputs such that the relation between the transformed inputs and outputs is as diagonal as possible. Then, decentralized control techniques are used to design independent SISO-controllers for the optimal decoupled system, which guarantee robust performance of the overall system. The complexity of this combination is comparable to that of a decentralized controller, but the performance approaches that of a full MIMO-controller. The optimal decoupling quality, and accordingly, the achievable closed loop performance depends on the symmetry in the system. Validation results on a automotive durability test rig simulation shows that the controller designed with decoupling yields better performance than a decentralized controller.**

I. INTRODUCTION

The design of a multiple-input-multiple-output (MIMO) model-based feedback controller suffers from two major problems. The first one is the identification step. The estimation of an accurate model, which matches well with the measured response, is often very cumbersome. Finding the optimal parametric MIMO-model, is still an important research topic ([1], [2]).

The second problem is the controller design. Most robust control techniques are well-suited for single-input-single-output (SISO) problems, but are, in practice, difficult to tune for MIMO-systems. Therefore, a decentralized controller is often used. A decentralized controller consist of independently designed SISO-controllers based on the diagonal elements of the system. The neglected off-diagonal elements in the MIMO-system limit the performance.

The control design procedure proposed in this paper tackles both problems. First an optimal frequency independent transformation of the inputs and outputs is calculated, such that the relation between the transformed inputs and transformed outputs is as diagonal as possible. This calculation is based on the measured frequency response function matrix (FRF-matrix), so no MIMO-identification is required. Secondly, a decentralized controller is designed between the transformed inputs and transformed outputs.

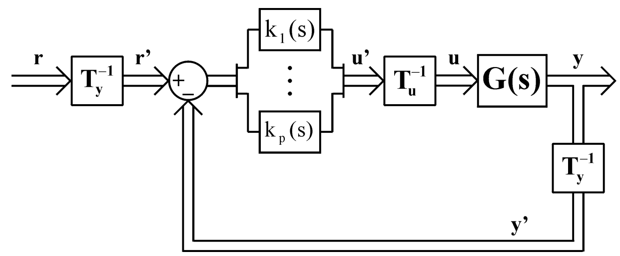

Fig. 1. Proposed control scheme: decoupling transformation of inputs and outputs, and p independent SISO-controllers.

This results in the control scheme of fig. 1. Robust stability of the total controller is guaranteed with a μ-synthesis-like treatment of the uncertainty of the measured FRF-matrix (due to measurement noise and nonlinearities) and the known model-error when the imperfectly decoupled system is approximated by a diagonal system.

The advantage with regard to decentralized control is that the main interactions in the system are taken into account, yielding better performance. The main advantage with regard to full MIMO-control is the simplicity of the design, including the fact that no MIMO-identification is required.

This paper is organized as follows: section II discusses the design of a decentralized controller for the decoupled system which guarantees robust performance. With respect to this robust performance criterium, the decoupling procedure, presented in section III, is an optimization that minimizes the interaction in the decoupled system. This procedure is validated on a non-linear simulation model of an axle test rig in section IV. Section V discusses the conclusions.

II. NOMINAL STABILITY AND ROBUST PERFORMANCE

The MIMO-controller is designed as a decentralized controller between the transformed inputs and outputs. The decentralized controller has to meet two criteria [3]: nominal stability (section II-B) and robust performance (section II-C). Nominal stability is achieved if the decentralized controller, designed for the diagonal elements of the decoupled system, is stable for the complete system. Robust performance is achieved if the performance requirements are met for all plants within the uncertainty set. This section summarizes the results of [3], and translates them to be used in the decoupling control scheme.

The nominal stability and robust performance criteria result in bounds on the sensitivity and complementary sensitivity of all independent SISO-control loops in the decentralized controller design, which can be used straightforwardly in an $\mathcal{H}_\infty$ loop shaping design of the SISO-controllers.

A. Nomenclature

$\tilde{\mathbf{G}}(f)$ is the measured MIMO-FRF-matrix at the frequency f, $\mathbf{T_Y}$ and $\mathbf{T_U}$ are the constant transformation matrices of the outputs (y) and the inputs (u) and $\tilde{\mathbf{G}}_\mathbf{d}(f)$ is the transformed measured FRF:

$$\tilde{\mathbf{G}}_\mathbf{d}(f) = \mathbf{T_Y}^{-1}\tilde{\mathbf{G}}(f)\mathbf{T_U}^{-1}. \tag{1}$$

$\tilde{\mathbf{D}}_\mathbf{d}(f)$ is defined as $diag\{\tilde{\mathbf{G}}_{\mathbf{d}_{ii}}(f)\}$ ($diag\{\ldots\}$ denotes the diagonal matrix consisting of the elements between braces). When the decoupling is perfect, $\tilde{\mathbf{G}}_\mathbf{d}(f)$ is equal to $\tilde{\mathbf{D}}_\mathbf{d}(f)$. In reality decoupling is seldom perfect, and in that case $\tilde{\mathbf{D}}_\mathbf{d}(f)$ is an approximation of $\tilde{\mathbf{G}}_\mathbf{d}(f)$. Finally, $\mathbf{D_d}(s)$ is a diagonal MIMO-model consisting of p independent parametric SISO-models: $\mathbf{D_d}(s) = \; diag\left\{d_{d_1}(s),\ldots,d_{d_p}(s)\right\}$.

The controller design discussed in this section is the design of a decentralized controller for $\tilde{\mathbf{G}}_\mathbf{d}(f)$, which consists of p independent SISO-controller designs based on $\mathbf{D_d}(s)$.

The uncertainty on the measured FRF $\tilde{\mathbf{G}}(f)$ is represented as multiplicative output uncertainty $\tilde{\mathbf{W}}_\mathbf{o}(f)$, which means that the true plant is unknown but is in the set $\left(\mathbf{I}+\tilde{\mathbf{W}}_\mathbf{o}(f)\mathbf{\Delta_o}(f)\right)\tilde{\mathbf{G}}(f)$ with $\|\mathbf{\Delta_o}\|_\infty < 1$. $\mathbf{C_d}(s) = diag\{k_1(s),\ldots,k_p(s)\}$ is the diagonal controller, designed for the system $\mathbf{D_d}(s)$. The complete controller which will be applied to the system $\tilde{\mathbf{G}}(f)$ is $\mathbf{C}(s) = \mathbf{T_U}^{-1}\mathbf{C_d}(s)\mathbf{T_Y}^{-1}$. The sensitivity and complementary sensitivity based on $\tilde{\mathbf{D}}_\mathbf{d}(f)$ and the independent SISO-controllers are defined as:

$$\begin{aligned} \tilde{\mathbf{S}}_\mathbf{d} &= (\mathbf{I}+\tilde{\mathbf{D}}_\mathbf{d}\mathbf{C_d})^{-1} \\ \tilde{\mathbf{T}}_\mathbf{d} &= (\mathbf{I}+\tilde{\mathbf{D}}_\mathbf{d}\mathbf{C_d})^{-1}\tilde{\mathbf{D}}_\mathbf{d}\mathbf{C_d}. \end{aligned} \tag{2}$$

Because $\tilde{\mathbf{D}}_\mathbf{d}$ and $\mathbf{C_d}$ are diagonal, $\tilde{\mathbf{S}}_\mathbf{d}$ and $\tilde{\mathbf{T}}_\mathbf{d}$ will be diagonal, which implies that:

$$\overline{\sigma}\left(\tilde{\mathbf{S}}_\mathbf{d}\right) = \max_{i=1,..,p}\left(\tilde{S}_{d,ii}\right) = \max_{i=1,..,p}\left((1+\tilde{D}_{d,ii}k_i)^{-1}\right) \tag{3}$$

The same holds for the complementary sensitivity. Applying the total controller to the system will result in the following sensitivity and complementary sensitivity:

$$\begin{aligned} \tilde{\mathbf{S}} &= (\mathbf{I}+\tilde{\mathbf{G}}_\mathbf{d}\mathbf{C_d})^{-1} &&= (\mathbf{I}+\tilde{\mathbf{G}}\mathbf{C})^{-1} \\ \tilde{\mathbf{T}} &= (\mathbf{I}+\tilde{\mathbf{G}}_\mathbf{d}\mathbf{C_d})^{-1}\tilde{\mathbf{G}}_\mathbf{d}\mathbf{C_d} &&= (\mathbf{I}+\tilde{\mathbf{G}}\mathbf{C})^{-1}\tilde{\mathbf{G}}\mathbf{C}. \end{aligned} \tag{4}$$

B. Nominal stability

Nominal stability is obtained if $\tilde{\mathbf{S}}$ is stable. Straightforward controller design result in the stability of $\tilde{\mathbf{S}}_\mathbf{d}$, but due to imperfect decoupling nominal stability is not guaranteed.

The easiest way to deal with this is to treat the differences between $\tilde{\mathbf{G}}_\mathbf{d}$ and $\tilde{\mathbf{D}}_\mathbf{d}$ as multiplicative output uncertainty:

$$\tilde{\mathbf{E}}_\mathbf{T}(f) = \left(\tilde{\mathbf{G}}_\mathbf{d}(f) - \tilde{\mathbf{D}}_\mathbf{d}(f)\right)\tilde{\mathbf{D}}_\mathbf{d}^{-1}. \tag{5}$$

Completely analogue to robust stability in standard $\mathcal{H}_\infty$-design, the decoupling controller is nominally stable if:

$$\overline{\sigma}\left(\tilde{\mathbf{T}}_\mathbf{d}(f)\right) < \left(\|\tilde{\mathbf{E}}_\mathbf{T}(f)\|_\infty\right)^{-1}. \tag{6}$$

This is condition is too conservative because $\tilde{\mathbf{E}}_\mathbf{T}(f)$ is not an uncertainty but a known error. [4] uses this knowledge to define a less conservative bound on the complementary sensitivity:

$$\overline{\sigma}\left(\tilde{\mathbf{T}}_\mathbf{d}(f)\right) < \mu_{C_d}^{-1}(\tilde{\mathbf{E}}_\mathbf{T}(f)). \tag{7}$$

The μ-norm is calculated with respect to the structure of the controller, which is diagonal.

Although (7) is a condition for the full MIMO-design, it can be used as an upper bound on the complementary sensitivity for all SISO-controller designs, due to (3). In this way, general nominal MIMO-stability conditions are translated to bounds of the complementary sensitivity of all SISO-control loops, which can be used in an $\mathcal{H}_\infty$-design of the SISO-controllers.

C. Robust performance

The uncertainty structure used in this paper is the multiplicative output uncertainty $\tilde{\mathbf{W}}_\mathbf{o}(f)$ of the measured FRF $\tilde{\mathbf{G}}(f)$. The equivalent uncertainty on $\tilde{\mathbf{G}}_\mathbf{d}(f)$ follows straightforwardly from (1):

$$\tilde{\mathbf{W}}_\mathbf{od} = \mathbf{T_Y}^{-1}\tilde{\mathbf{W}}_\mathbf{o}\mathbf{T_Y}. \tag{8}$$

Robust performance (RP) is achieved if the controller satisfies the performance specification for all plants within the set $\left(\mathbf{I}+\tilde{\mathbf{W}}_\mathbf{od}(f)\mathbf{\Delta_o}(f)\right)\tilde{\mathbf{G}}_\mathbf{d}(f)$ with $\|\mathbf{\Delta_o}\|_\infty < 1$. Fig. 2 shows the scheme used to design such a controller. The performance weight $\mathbf{W_p}$ defines the performance criterium: $\|\mathbf{W_p S}\|_\infty < 1$. This scheme can be transformed in the general μ-analysis structure of fig. 3. $\mathbf{\Delta_o}$ defines the structure of the uncertainty, $\mathbf{\Delta_p}$ is a full matrix stemming from the $\mathcal{H}_\infty$ performance specification.

The RP-condition as a function of $\mathbf{M}$ is:

$$\mu_{\mathbf{\Delta}}(\mathbf{M}) < 1, \qquad \forall f \tag{9}$$

with μ calculated with respect to the structure of $\mathbf{\Delta} \;=\; diag\{\mathbf{\Delta_o},\mathbf{\Delta_p}\}$. Applying μ-synthesis to design RP-controllers would again require that $\tilde{\mathbf{E}}_\mathbf{T}$ is treated as uncertainty, yielding a too conservative controller.

[3] describes a method to deal with this problem. In order to apply that method the interconnection matrix $\mathbf{M}$ is written as a lower linear fractional transformation of $\tilde{\mathbf{S}}_\mathbf{d}$ and $\tilde{\mathbf{T}}_\mathbf{d}$:

$$\begin{aligned} \mathbf{M} &= \mathbf{N}_{\mathbf{11}}^{\mathbf{T_d}} + \mathbf{N}_{\mathbf{12}}^{\mathbf{T_d}}\tilde{\mathbf{T}}_\mathbf{d}\left(\mathbf{I}-\mathbf{N}_{\mathbf{22}}^{\mathbf{T_d}}\tilde{\mathbf{T}}_\mathbf{d}\right)^{-1}\mathbf{N}_{\mathbf{21}}^{\mathbf{T_d}} \\ \mathbf{M} &= \mathbf{N}_{\mathbf{11}}^{\mathbf{S_d}} + \mathbf{N}_{\mathbf{12}}^{\mathbf{S_d}}\tilde{\mathbf{S}}_\mathbf{d}\left(\mathbf{I}-\mathbf{N}_{\mathbf{22}}^{\mathbf{S_d}}\tilde{\mathbf{S}}_\mathbf{d}\right)^{-1}\mathbf{N}_{\mathbf{21}}^{\mathbf{S_d}}. \end{aligned} \tag{10}$$

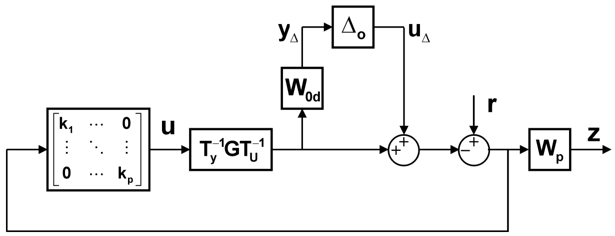

Fig. 2. Multiplicative output uncertainty, for robust controller design with decoupling.

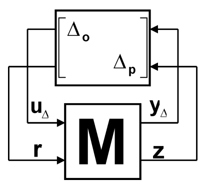

Fig. 3. General structure for controller design with robust performance.

The matrices $\mathbf{N_{ij}^{T_d}}$ and $\mathbf{N_{ij}^{S_d}}$ are independent of $\mathbf{C_d}$. According to [3], the RP-criterium (9) can now be written as follows:

$$\bar{\sigma}(\tilde{\mathbf{S}}_\mathbf{d}) \leq \tilde{c}_{\mathbf{S_d}} \quad \textbf{or} \quad \bar{\sigma}(\tilde{\mathbf{T}}_\mathbf{d}) \leq \tilde{c}_{\mathbf{T_d}} \quad \forall f, \tag{11}$$

with $\tilde{c}_{\mathbf{S_d}}$ the solution of the following equations:

$$\mu_{\hat{\mathbf{\Delta}}}\left(\left[\begin{array}{cc} \mathbf{N_{11}^{S_d}} & \mathbf{N_{12}^{S_d}} \\ \tilde{c}_{\mathbf{S_d}}\mathbf{N_{21}^{S_d}} & \tilde{c}_{\mathbf{S_d}}\mathbf{N_{22}^{S_d}} \end{array}\right]\right) = 1. \tag{12}$$

The structure $\hat{\mathbf{\Delta}}$ used in this μ-norm calculation is $diag\{\mathbf{\Delta}, \mathbf{C_d}\}$. Calculation of $\tilde{c}_{\mathbf{T_d}}$ is completely analogue. Remark that (11) states that at each frequency only one of both conditions must be satisfied.

The obtained RP-criterium is a sufficient but not necessary condition for robust performance. It is however the tightest bound possible [3]. This means that there can exist decentralized controllers which violate the bounds and still have robust performance, but at the same time there will exist controllers with the same values for $\bar{\sigma}(\tilde{\mathbf{S}}_\mathbf{d})$ and $\bar{\sigma}(\tilde{\mathbf{T}}_\mathbf{d})$ which do not yield robust performance.

In the case of multiplicative output uncertainty, the interconnection matrix $\mathbf{M}$ can be calculated from fig. 2 and the RP-bounds $\tilde{c}_{\mathbf{S_d}}$ and $\tilde{c}_{\mathbf{T_d}}$ can be calculated as the solution of:

$$\mu_{\hat{\mathbf{\Delta}}}\left[\begin{array}{ccc} -\tilde{\mathbf{W}}_\mathbf{od} & \tilde{\mathbf{W}}_\mathbf{od} & \tilde{\mathbf{W}}_\mathbf{od} \\ 0 & 0 & -\mathbf{W_p} \\ \tilde{c}_{\mathbf{S_d}}\tilde{\mathbf{D}}_\mathbf{d}\tilde{\mathbf{G}}_\mathbf{d}^{-1} & -\tilde{c}_{\mathbf{S_d}}\tilde{\mathbf{D}}_\mathbf{d}\tilde{\mathbf{G}}_\mathbf{d}^{-1} & \tilde{c}_{\mathbf{S_d}}\tilde{\mathbf{E}}_\mathbf{S} \end{array}\right] = 1, \tag{13}$$

with $\tilde{\mathbf{E}}_\mathbf{S} = \left(\tilde{\mathbf{G}}_\mathbf{d} - \tilde{\mathbf{D}}_\mathbf{d}\right)\tilde{\mathbf{G}}_\mathbf{d}^{-1}$ and:

$$\mu_{\hat{\mathbf{\Delta}}}\left[\begin{array}{ccc} 0 & 0 & \tilde{\mathbf{W}}_\mathbf{od}\tilde{\mathbf{G}}_\mathbf{d}\tilde{\mathbf{D}}_\mathbf{d}^{-1} \\ -\mathbf{W_p} & \mathbf{W_p} & -\mathbf{W_p}\tilde{\mathbf{G}}_\mathbf{d}\tilde{\mathbf{D}}_\mathbf{d}^{-1} \\ -\tilde{c}_{\mathbf{T_d}}I & \tilde{c}_{\mathbf{T_d}}I & -\tilde{c}_{\mathbf{T_d}}\tilde{\mathbf{E}}_\mathbf{T} \end{array}\right] = 1. \tag{14}$$

The last step in the controller design is to find a controller which meets at every frequency at least one of the conditions of (11). Due to (3), the boundaries must be met by every SISO-controller. Both boundaries on the SISO-sensitivity and SISO-complementary sensitivity, define in fact an upper and lower bound on each diagonal element of the open loop transfer function:

$$\begin{array}{l} |\tilde{S}_{d,ii}| \leq \tilde{c}_{\mathbf{S_d}} \Rightarrow |\tilde{D}_{d,ii}k_i| > \left|\frac{1}{\tilde{c}_{\mathbf{S_d}}}\right| - 1 \\ |\tilde{T}_{d,ii}| \leq \tilde{c}_{\mathbf{T_d}} \Rightarrow |\tilde{D}_{d,ii}k_i| < \frac{1}{\left|\frac{1}{\tilde{c}_{\mathbf{T_d}}}\right| - 1} \text{ if } |\tilde{c}_{\mathbf{T_d}}| > 1. \end{array} \tag{15}$$

The plot of both constraints is a simple visual check to see if it is possible to meet the constraints and it gives an idea in which frequency band each RP-bound will be active.

III. DECOUPLING PROCEDURE

A. Introduction

Many decoupling procedures have been developed in the past. The easiest-to-use class of decoupling methods is based on matrix-decompositions. MacFarlane [5] introduces in 1970 the so-called *commutative controller*, based on an eigenvalue decomposition. In 1982 Hung [6] launched a controller based on the singular value decomposition. The decomposition as proposed in (1), puts no constraints on the transformation matrices $\mathbf{T_U}$ and $\mathbf{T_Y}$. If eigenvalue or singular value decompositions are used, some constraints are inherent in the used method: in the eigenvalue decomposition the left and right transformation matrices are the inverse of each other, in the singular value decomposition the left and right transformation matrices are unitary matrices.

A general decoupling transformation is described in the theory of the *Dyadic Transfer function Matrices* (DTM). A $p \times p$ transfer function matrix $\mathbf{G}(s)$ is called dyadic if there exist constant $p \times p$ matrices $\mathbf{T_U}$ and $\mathbf{T_Y}$ and rational transfer functions $g_1(s), \ldots, g_p(s)$ such that:

$$\mathbf{G}(s) = \mathbf{T_Y} diag\{g_1(s), \ldots, g_p(s)\}\mathbf{T_U}. \tag{16}$$

Owens [7] showed that if $\mathbf{G}(s)$ is dyadic, the columns of $\mathbf{T_Y}$ can be calculated as the eigenvectors of $\mathbf{G}(c_2)\mathbf{G}^{-1}(c_1)$ and the columns of $\mathbf{T_U^{-1}}$ as the eigenvectors of $\mathbf{G}^{-1}(c_1)\mathbf{G}(c_2)$ with c_1 and c_2 two arbitrary constants. If a system is dyadic, the calculated transformation matrices are real and independent of the chosen constants. If the transformation found with this procedure is not real, the system is not dyadic. In that case, the transformation matrices do not decouple the system perfectly.

It is obvious that only few systems are dyadic. Perfect symmetry is required and so, in practice, Owens' method is hardly usable. The method to calculate the transformation matrices in this paper is an optimization of the elements of $\mathbf{T_U}$ and $\mathbf{T_Y}$. Next section discusses the choice of the cost function. Section III-C describes the calculation of an initial estimate, required to start the optimization procedure.

B. Optimization procedure

With p the number of inputs and outputs, $\mathbf{T_U}$ and $\mathbf{T_Y}$ have $2p^2$ elements. Multiplying a row of $\mathbf{T_U}$ or a column of $\mathbf{T_Y}$ with any nonzero number, does not influence the decoupling quality, yielding $2p(p-1)$ parameters left to optimize. Due to these many optimization parameters, the cost function should be easy to calculate.

The goal of the decoupling procedure is to simplify the controller design afterwards. If the decoupling is not accurate, the RP-bounds will be very difficult to meet. The best optimization criterium would be an optimization of the RP-bounds $\tilde{c}_{\mathbf{S_d}}$ (13) and $\tilde{c}_{\mathbf{T_d}}$ (14). This is however not realistic because the calculation of these bounds takes a few minutes.

The RP-bounds are mainly determined by the differences between $\tilde{\mathbf{G}}_\mathbf{d}(f)$ and $\tilde{\mathbf{D}}_\mathbf{d}(f)$. That is why the relative difference $\tilde{\mathbf{E}}_\mathbf{T}$ between $\tilde{\mathbf{G}}_\mathbf{d}$ and $\tilde{\mathbf{D}}_\mathbf{d}$ is used in the optimization procedure as follows (which is also an optimization of the nominal stability criterium (6)):

$$\min_{\mathbf{T_U},\mathbf{T_Y}} \left\{ \max_f \left[\bar{\sigma}(\tilde{\mathbf{E}}_\mathbf{T}(f,\mathbf{T_U},\mathbf{T_Y}))W_f(f) \right] \right\}. \qquad (17)$$

$W_f(f)$ is a frequency dependent weighting function. Accurate decoupling is most important around the cross-over frequency. In order to avoid that, in that frequency range, $\tilde{\mathbf{S}}$ would peak a lot and differ too much from $\tilde{\mathbf{S}}_\mathbf{d}$, $W_f(f)$ can be made larger in that frequency band.

C. Initial estimate

The optimization procedure of the previous section is non-convex, and a lot of parameters must be optimized, so an accurate initial estimate is necessary.

Owens' method is used to calculate this initial estimate. Because no MIMO-model is available, c_1 and c_2 must be chosen as two frequencies f_1 and f_2 where the FRF is measured. The transformation matrices $\mathbf{T_Y}$ and $\mathbf{T_U}^{-1}$ can then be calculated as the eigenvectors of $\tilde{\mathbf{G}}(f_2)\tilde{\mathbf{G}}^{-1}(f_1)$ and $\tilde{\mathbf{G}}^{-1}(f_1)\tilde{\mathbf{G}}(f_2)$ respectively, for each pair of available frequencies f_1 and f_2 [8].

One problem encountered when applying Owens' procedure to a system which is not dyadic, is the fact that the calculated transformation matrices are complex, and therefore cannot be used to transform the time-domain signals as in the control scheme of fig. 1. The ALIGN-method [5] is used to find the real matrices which match best with the complex transformation matrices.

A second problem is caused by the fact that the transformation matrices are not unique anymore if the system is not dyadic: the decoupling quality strongly depends on the choice of f_1 and f_2. To obtain the optimal choice of f_1 and f_2 the following optimization procedure is used (with $\mathcal{F}$ the set of all frequencies where the FRF is measured):

$$\min_{f_1,f_2\in\mathcal{F},f_1\neq f_2} \left\{ \max_f \left[\bar{\sigma}(\tilde{\mathbf{E}}_\mathbf{T}(f,f_1,f_2))W_f(f) \right] \right\}. \qquad (18)$$

This optimization is of course completely analogue to (17), but here the global optimum is easy to find because f_1 and f_2 has to be chosen out of the finite set $\mathcal{F}$.

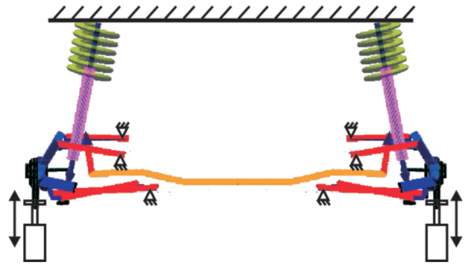

Fig. 4. Axle test rig.

IV. SIMULATION RESULTS

Fig. 4 is a schematic representation of a durability test rig for one axle of a car. The points of the axle and the suspensions which are normally connected to the car body are fixed on this test rig. The wheels are mounted on two position-controlled hydraulic actuators. The inputs of the system are the signals sent to these actuators, the outputs are the accelerations measured on each wheel. To make the vibration tests representative for the further life-time of the axle, reference signals, for each output, are measured during a test drive on a test track. These reference signals have to be reproduced on the test rig as accurately as possible.

The calculation of the control signals for the hydraulic actuators, such that the measured signals on the test rig match the reference signals, is a MIMO-tracking problem. Current industry practice to solve this problem, is to use an off-line iterative process [10]. [10] shows that extending the current process with a high-performance MIMO-controller, allows to reduce the number of iterations significantly.

The system in this example is a numerical nonlinear simulation model of the test rig of fig. 4. Nonlinear stiffness and damping are used to model the nonlinearities in the test rig. The axle test rig is not perfectly symmetric due to an asymmetric mass distribution, differences in suspension characteristics and different PID-settings for the left and right actuator. A perfect symmetrical axle test rig would be dyadic.

First, the performance of decentralized control, without decoupling, is analyzed. The performance requirement used in this section is shown as the dotted line in fig. 5. $\tilde{c}_{\mathbf{S_d}}$ (full line) and $\tilde{c}_{\mathbf{T_d}}$ (dashed line) are the resulting RP-bounds which have to be met by the independent SISO-designs. Remark that at each frequency, only one bound must be met (11). Transforming these RP-bounds to an upper and lower bound on the open loop transfer function (15) shows that the RP-bounds are impossible to meet (fig. 6). A proper open loop transfer function has to meet $\tilde{c}_{\mathbf{S_d}}$ at low and $\tilde{c}_{\mathbf{T_d}}$ at high frequencies. In an intermediate frequency range, however, neither $\tilde{c}_{\mathbf{S_d}}$ nor $\tilde{c}_{\mathbf{T_d}}$ can be met.

Secondly the system is decoupled with the procedure of section III. A first optimization is performed with a simple first order weighting function $W_{f,1}$ used in (17). Fig. 7 shows $|W_{f,1}|$ (full line) together with the obtained decoupling quality $\|\mathbf{E}_{\mathbf{T},\mathbf{1}}\|_\infty$ (dashed line). Around the cross-over frequency (≈ 15 Hz) $\|\mathbf{E}_{\mathbf{T},\mathbf{1}}\|_\infty$ rises to 0.5. This

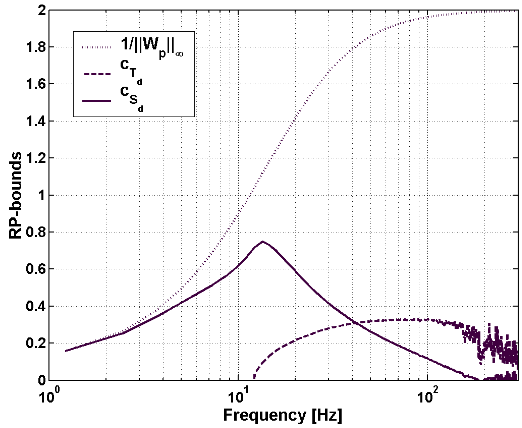

Fig. 5. RP-bounds for decentralized control of axle test rig: performance specification $\|\frac{1}{W_p}\|_\infty$ (dotted line), RP-bounds $\tilde{c}_{\mathbf{S_d}}$ (full line) and $\tilde{c}_{\mathbf{T_d}}$ (dashed line).

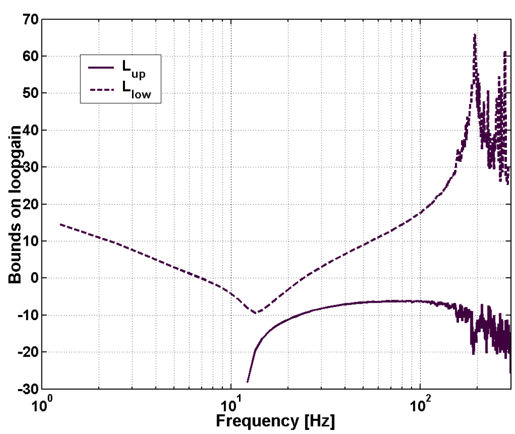

Fig. 6. Boundaries on open loop transfer function due to RP-bounds: upper bound (full line), lower bound (dashed line).

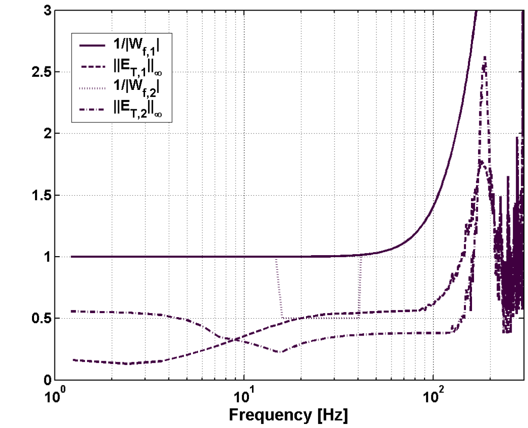

Fig. 7. Decoupling results: $|W_{f,1}|$ used in first decoupling optimization (full line) and resulting difference between $\tilde{\mathbf{G}}_{\mathbf{d}}$ and $\tilde{\mathbf{D}}_{\mathbf{d}}$: $\|\mathbf{E_{T,1}}\|_\infty$ (dashed line). $|W_{f,2}|$ (dotted line) and $\|\mathbf{E_{T,2}}\|_\infty$ (dash-dotted line) are the same for the second decoupling optimization.

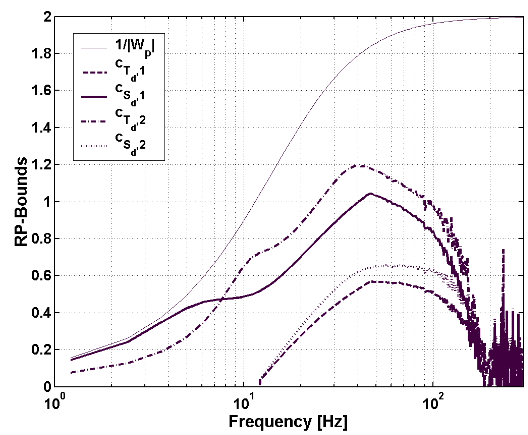

Fig. 8. RP-bounds with decoupling control: performance specification $\|\frac{1}{W_p}\|_\infty$ (thin full line), RP-bounds $\tilde{c}_{\mathbf{S_d},\mathbf{1}}$ (full line) and $\tilde{c}_{\mathbf{T_d},\mathbf{1}}$ (dashed line) for first decoupling results, RP-bounds $\tilde{c}_{\mathbf{S_d},\mathbf{2}}$ (dash-dotted line) and $\tilde{c}_{\mathbf{T_d},\mathbf{2}}$ (dotted line) for second decoupling results.

large difference between $\tilde{\mathbf{G}}_{\mathbf{d}}$ and $\tilde{\mathbf{D}}_{\mathbf{d}}$ yields an upper bound on the sensitivity which is hard to meet. These RP-bounds ($\tilde{c}_{\mathbf{S_d},\mathbf{1}}$ and $\tilde{c}_{\mathbf{T_d},\mathbf{1}}$) are plotted in fig. 8. $\tilde{c}_{\mathbf{S_d},\mathbf{1}}$ equals 1 around 40Hz, which means that SISO-controllers with a bandwidth of 40 Hz are required to obtain a robust MIMO-bandwidth of 15 Hz.

To improve the decoupling quality around cross-over a second weighting function $W_{f,2}$ is used (dotted line in fig. 7). $W_{f,2}$ is equal to $W_{f,1}$, except between 15 and 40 Hz where $W_{f,2}$ equals 2. The obtained decoupling quality (dash-dotted line) is indeed improved around cross-over, but is worse at low frequencies. The RP-bounds are the dash-dotted and dotted line in fig. 8. As expected, the RP-bound $\tilde{c}_{\mathbf{S_d},\mathbf{2}}$ around cross-over is less severe than $\tilde{c}_{\mathbf{S_d},\mathbf{1}}$. At low frequencies however, the performance of the SISO-controllers will have to be somewhat better to meet the RP-bounds.

The upper bound and lower bound on the open loop transfer function (15) plotted in fig. 9 shows that a controller which satisfies $\tilde{c}_{\mathbf{S_d},\mathbf{2}}$ up to 20 Hz, and $\tilde{c}_{\mathbf{T_d},\mathbf{2}}$ at higher frequencies meets at every frequency one of both conditions and will have robust performance. After identification of the diagonal elements of $\tilde{\mathbf{G}}_{\mathbf{d}}$, $\mathcal{H}_\infty$ mixed sensitivity loop shaping is used to design the SISO-controllers. Simple first order weighting function are fitted on $\tilde{c}_{\mathbf{S_d},\mathbf{2}}$ ($< 20Hz$) and $\tilde{c}_{\mathbf{T_d},\mathbf{2}}$ ($> 20Hz$). In fig. 10 the sensitivity $\tilde{\mathbf{S}}_{\mathbf{d}}$ (dashed line) and complementary sensitivity $\tilde{\mathbf{T}}_{\mathbf{d}}$ (dash-dotted line) are plotted together with the RP-bounds. At some frequencies the bounds are slightly violated. The amplitude of the open loop transfer functions of both controllers is plotted in fig. 9 (dotted and dash-dotted line which lie almost on top of each other).

To check the robust performance of the total controller, a μ-analysis of the total control scheme (fig. 2) is performed. The μ-norm (fig. 11) is less than one at all frequencies which guarantees robust performance. Nominal stability can be easily checked with (7).

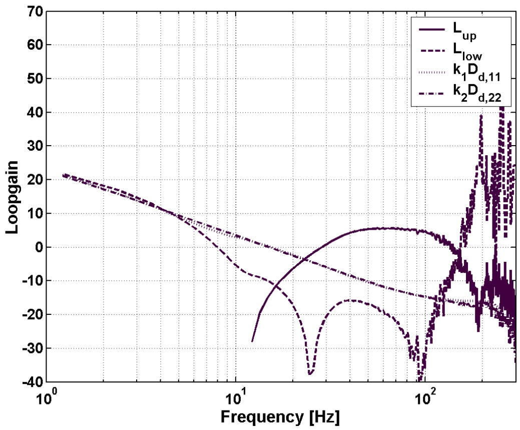

Fig. 9. Boundaries on open loop transfer function due to RP-bounds for second decoupling results: upper bound (full line), lower bound (dashed line), together with the designed open loop transfer functions: $\tilde{D}_{d,11}k_1$ (dotted line) and $\tilde{D}_{d,22}k_2$ (dash-dotted line) which are almost equal.

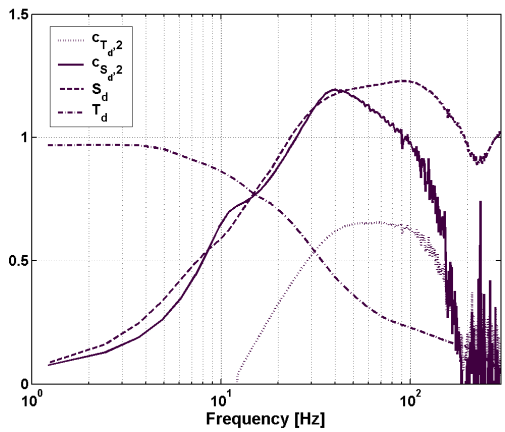

Fig. 10. Designed $\tilde{\mathbf{S}}_{\mathbf{d}}$ (dashed line) and $\tilde{\mathbf{T}}_{\mathbf{d}}$ (dash-dotted line) together with the RP-bounds $\tilde{c}_{\mathbf{S_d},\mathbf{2}}$ (full line) and $\tilde{c}_{\mathbf{T_d},\mathbf{2}}$ (dotted line) for the second decoupling results.

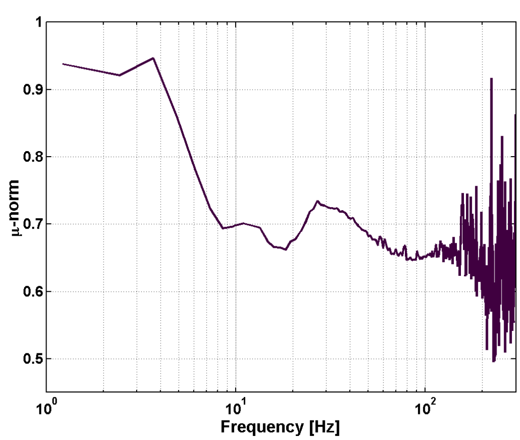

Fig. 11. Final-validation: μ-analysis of complete closed-loop system.

V. CONCLUSION

This paper describes a control strategy applicable to square MIMO-systems with a certain degree of symmetry. First the decoupling step is an optimization of the transformation of inputs and outputs, such that the relation between the transformed inputs and outputs is as diagonal as possible. In the controller design step, decentralized control is used to control the nearly decoupled system. Bounds for sensitivities and complementary sensitivities of the different SISO-controllers are derived which guarantee robust performance of the total controller. A method is proposed to obtain useful weighting functions (for SISO-$\mathcal{H}_\infty$ design) from these RP-bounds.

Thanks to the decoupling transformation, the main interactions are taken into account in the control design, yielding a better performance of the total MIMO-controller than the performance of a decentralized controller.

ACKNOWLEDGEMENTS

This research is sponsored by the Belgian programme on Interuniversity Poles of Attraction, initiated by the Belgian State, Prime Minister's Office, Science Policy Programming (IUAP). D. Vaes is a Research Assistant of the Fund for Scientific Research (F.W.O.) - Flanders (Belgium). The scientific responsibility remains with its authors. We would like to thank J. De Cuyper from LMS International for the use of his simulation models of an axle test rig.

REFERENCES

[1] T. McKelvey, *Identification of State-Space Models from Time and Frequency Data*, Linköping Studies in Science and Technology, Linköping (1995).

[2] P. Van Overschee, B. De Moor, *Subspace Identification for Linear Systems: Theory, Implementation, Applications*, Kluwer Academic Publishers (1996).

[3] S. Skogestad, M. Morari, *Robust Performance of Decentralized Control Systems by Independent Designs* Automatica, Vol. 25 (1) (1989).

[4] P. Grosdidier, M. Morari, *Interaction measures for systems under decentralized control*, Automatica, Vol. 22 (3), pp. 309-319 (1986).

[5] A. G. J. MacFarlane, *Commutative controller: A new technique for the design of multivariable control systems*, Electronic letters, Vol. 6 (1970), pp. 121-123.

[6] Y. S. Hung, A. G. J. MacFarlane, *Multivariable feedback: A quasi-classical approach*, Springer-Verlag (1982).

[7] D. H. Owens, *Feedback and multivariable systems*, Peter Peregrinus Ltd (1978).

[8] D. Vaes, W. Souverijns, J. De Cuyper, J. Swevers, P. Sas, *Optimal decoupling for improved multivariable controller design, applied on an automotive vibration test rig*, in *Proceedings of the ACC Conference, Denver (Colorado), USA, 2003, June 4-6*, pp. 785-790.

[9] S. Skogestad, I. Postlethwaite *Multivariable Feedback Control, Analysis and Design*, John Wiley and Sons (1996).

[10] J. De Cuyper, M. Verhaegen, J. Swevers, *Off-line Feed-forward and $\mathcal{H}_\infty$ Feedback Control for improved Tracking on an industrial vibration test rig*, Journal of Control Engineering Practice, Vol 11, pp. 129-140 (2003)